

Design of Belt Sprinkler Monitoring System Based on Image Processing Technology

Wenzhu Wang, Shaochuan Xu, and Yue Teng

Abstract—Belt conveyor belts have a wide range of applications in the transportation of materials, and the phenomenon of deviation and material spillage may occur in the process of conveying materials. However, the method of manually checking faults is not real-time and inefficient. If it cannot be discovered and handled in time, it will cause greater failures and waste of materials, and bring huge economic losses. In response to these problems, this paper designs a belt sprinkler monitoring system based on image processing. First, the real-time image of the belt transportation status is collected through the camera, and the edge position of the belt is identified by the Hough line detection method. Through the expansion, corrosion and binarization of the image, the characteristics of the distribution state of the mineral material on the belt are obtained. Then build the SVM sprinkling forecast model, select the pixel value of each point on the profile line as the input, and forecast the belt running state. The experimental results show that SVM shows good classification and recognition effect and generalization ability. The system has certain accuracy, real-time and high efficiency for the detection of belt running status. The system has a certain degree of accuracy, real-time and high efficiency in the detection of the belt running status. It can realize the real-time warning of belt deviation and sprinkling, thereby reducing the accident rate, ensuring the efficient work of the conveyor belt, and reducing unnecessary losses.

Index Terms—Belt conveyor; Image processing; Deviation detection; Support vector machine; Sprinkling detection

I INTRODUCTION

The belt conveyor belt has the characteristics of large transportation volume and sustainable transportation; it is suitable for transporting various forms of goods, and has been widely used in modern mine transportation of mineral materials. The belt mainly relies on friction to transmit power, so it is prone to failure. One of the most common faults is the deviation of the conveyor belt. In practical applications, belt conveyors are prone to belt deviation due to the installation environment and the heavy weight of the transport materials. If it is not controlled in time, it is easy to cause mineral materials to spill out. If the spilled mineral material enters the conveyor belt, the conveyor belt is prone

to failure, which will increase the difficulty of belt maintenance and reduce the efficiency of the belt. However, due to the complex on-site environment and the relatively large area of the work area, manual inspection methods are often not real-time. When the operator discovers that the belt is off-track, in most cases it has caused greater failures and caused greater losses^[1]. In addition, materials are often spilled when the belt is deflected, which can easily cause safety accidents. In the process of patrol inspection by operators, the safety of personnel cannot be guaranteed. Therefore, it is necessary to design a system for detecting belt deviation and sprinkling, thereby reducing losses and reducing the incidence of safety accidents.

Some scholars have conducted research on belt deviation detection, such as: Mengchao Zhang et al. used laser technology to build a conveyor belt deviation detection system^[2]. Chan Zeng and Junfeng Zheng et al. proposed a real-time conveyor belt detection algorithm based on multi-scale feature fusion networks^[3]. Yanli Yang and Changyun Miao et al. proposed a fast image segmentation algorithm to process belt images online, and detect longitudinal cracks and belt deviations from binary seat belt images.^[4] Zhu Liang Li Dongbo Wu Chongyou Wu Shaofeng Yuan Yanqiang used regression analysis methods such as support vector machine (SVM) and extreme learning machine (ELM), and took the deviation features extracted by LTSA+GRNN and CDBN as input to establish an online prediction model for belt deviation^[5]. Qiu Yi Chu et al. obtained the belt idling speed and belt speed by theoretical analysis and numerical simulation analysis, and provided theoretical guidance for the deviation correction and prevention of belt conveyor^[6]. The existing belt deviation detection method mainly detects the belt deviation, but ignores the influence of ore distribution on the belt deviation.

In response to the above problems, this paper studies a method for detecting sprinkling of belt conveyors based on image processing, which can monitor the running status of the belt in real time. The contribution of this article is: A method of gray-scale processing and filtering for image denoising is proposed. Hough line detection is used to detect the edge of the belt, and then the image is corroded, expanded and binarized to obtain the state distribution of the transported minerals on the belt. After that, the relationship between various data on the belt is mathematically modeled to compare the distance between the position of the belt when the belt is empty and the position when the belt is loaded to determine whether the belt is running off the track. On the basis of traditional classification methods, machine learning methods are used, and SVM sprinkling forecast models are constructed to finally realize fault detection and classification report early warning for belt deviation and sprinkling. The

Manuscript received April 15, 2021; revised December 3, 2021.

Wenzhu Wang is a Postgraduate Student of School of Control Science and Engineering, University of Science and Technology Liaoning, Anshan, 114051 China. (e-mail: w1599751883@163.com).

Shaochuan Xu is an Associate Professor of School of Control Science and Engineering, University of Science and Technology Liaoning, Anshan, 114051 China. (corresponding author, phone: 86-0412-5929747; e-mail: shaochuanxu1@163.com).

Yue Teng is a Postgraduate Student of School of Control Science and Engineering, University of Science and Technology Liaoning, Anshan, 114051 China. (e-mail: 877811919@qq.com).

system has been tested and applied in the mine field and achieved good results.

II CAUSE ANALYSIS AND BASIC SYSTEM COMPOSITION

A. Analysis of the causes of belt deviation

In the process of using belts to transport mineral materials, belt deviations often occur. Sometimes the belt will resume normal operation when there is no load, and sometimes there will be greater failures. After analysis, it is found that the reasons for the belt deviation are roughly as follows: the deceleration shaft is broken due to overload operation; the transport material falls into the machine and the roller is damaged; the uneven distribution of the transported mineral material causes the tension of the belt to be different, which makes the belt Deviation and mineral fall [7]. Therefore, in the actual application process, the distribution state of the transported mineral material on the belt will also have a great impact on the running state of the belt to a certain extent. Therefore, while detecting whether the belt is off-track, it is also necessary to pay more attention to the distribution of mineral materials on the belt surface and the problem of mineral spillage caused by belt off-tracking.

B. Basic structure of the system

First, it is necessary to install cameras in different sections of different belts in the workshop to collect the working status of different sections of belts in different positions in real time. The system obtains images of the belt surface at different positions through the video captured by the camera, and then analyzes and processes the data to determine whether the belt is misaligned and the degree of misalignment of the belt. Then, by processing the captured images, the areas with mineral material and those without mineral material are classified to further determine whether the belt has spilled material. The system monitors the status of the belt in real time. Once the belt's running status is found to be abnormal, the alarm processing device will be activated immediately; the operator can see the running status of the belt at different locations and the system's judgment result of the corresponding status on the monitoring screen.

The system designed in this paper mainly includes: image acquisition and preprocessing module, belt deviation judgment and belt sprinkling judgment module, and early warning module. The image acquisition and processing module converts the collected video and images into digital signals; the belt deviation judgment and belt sprinkling judgment module analyze and processes the data obtained by image processing; then the results of the above two judgments are used in the early warning It is displayed in the module, and an alarm is given to the abnormal belt. The system function module is shown in Fig. 1

III IMAGE PREPROCESSING

A. Image grayscale processing and filtering, denoising

The work site environment is very complicated, and the quality of the video and image captured by the camera will be subject to a lot of external interference and internal

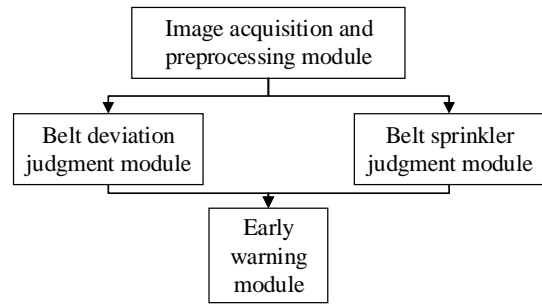


Fig. 1. System function modules

The basic flow chart of system work is shown as in Fig. 2.

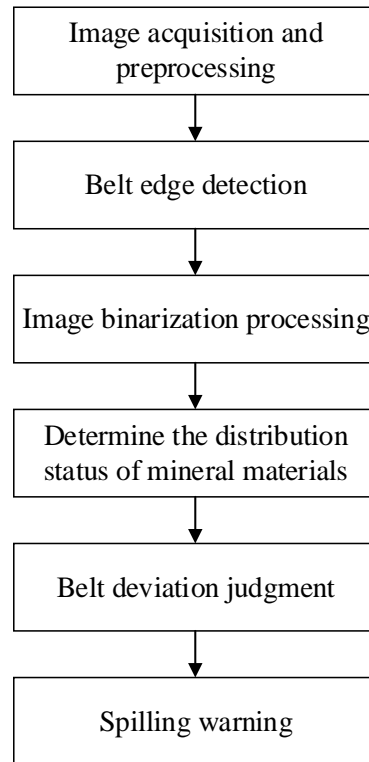


Fig. 2. System flow chart

interference. These interferences will overwhelm the salient features of the image, which is not conducive to the extraction of image features. Therefore, the image needs to be processed: the intercepted image is grayed out, that is, the three components of *R*, *G*, and *B* are reasonably weighted and weighted and summed to obtain the gray value. The gray weight value selected by this system is

$$Gray = 0.3R + 0.5G + 0.1B \tag{1}$$

Where *R*, *G*, and *B* represent the red, green, and blue components respectively.

Then use NI VISION software to filter and denoise the gray-scaled image. When dust adheres to the camera lens in the processing workshop, spots will be formed, and the video imaging and transmission process may also be contaminated by noise. During the imaging process, these interferences may appear on the image in the form of spots, which are not conducive to the analysis of image features. So it is necessary to preprocess the collected images [8].

B. Image binarization processing

In the process of using belts to transport mineral materials, mineral materials are mainly distributed in the middle of the belt. There is a certain gray level difference between the mineral material area and the mineral material area on the image, so it is necessary to process the detected belt image:

- 1) Binarization processing. In order to better distinguish the mineralized area and the mineral-free area on the image, the image needs to be binarized to convert the grayscale image to a black and white image, and then use the moment preservation method to select a suitable binarization threshold, and finally get the processed binary image.
- 2) Expand and corrode the image. In order to obtain an image that is more conducive to subsequent operations, it is necessary to remove the interference of the external environment to the image as much as possible through the above steps, so that there is a certain continuous area on the image^[9].

Fig. 3 shows the image after binarization, expansion, and corrosion. The light-colored area in the figure indicates the area without minerals, and the dark area indicates the area with minerals. From the figure, we can see that there is a certain width of light-colored area at the edge of the belt. It can be seen that this area is not covered by mineral material, indicating that there is a distance between the mineral material on the belt and the edge of the belt.

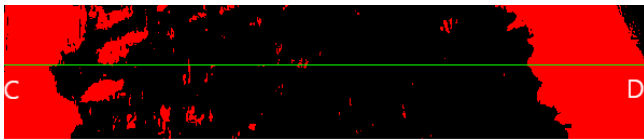


Fig. 3. Binarized image and selected target line

Draw a cross-sectional diagram on the image after the above processing, as shown in Fig. 3. That is, select two points C and D on the left and right ends of the belt on the image, connect the two points to form a target straight line, and obtain the pixel values of all points on the straight line.

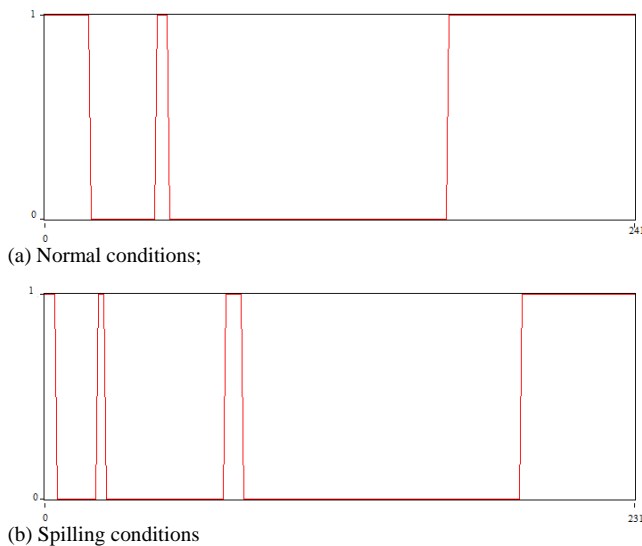


Fig. 4. The pixel value profile on the target line

In Fig. 4(a), the abscissa represents the pixel coordinates on the target straight line, the ordinate represents the pixel value, a pixel value of 0 indicates an area with minerals, and a pixel value of 1 indicates an area without minerals. It can be seen from the figure that the widths of area I and area II are both within the appropriate range and the difference is small. Some small mineral-free areas in the middle area of the belt, that is, the mineral-concentrated area, can be regarded as interference and can be ignored, fig. 4 (b) is the profile of pixel value in the spraying state.

IV BELT EDGE DETECTION AND DEVIATION JUDGMENT

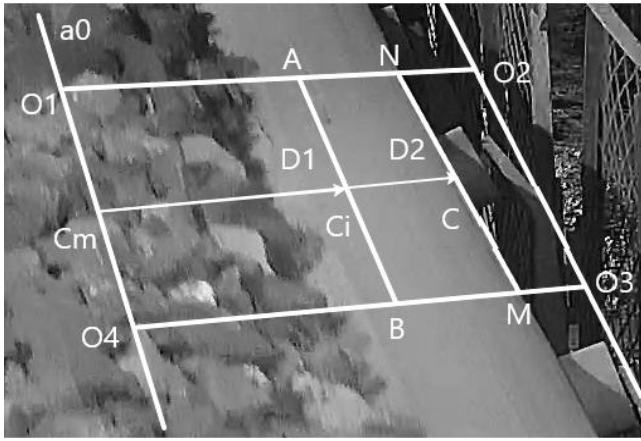
A. Analysis of belt identification area

First, select the ROI area in the pre-processed image, select the ideal middle position of the belt width and the maximum position of the belt deviation to establish a standard straight line, the slope of which is the direction of belt movement, that is, the straight line a_0 , a_1 shown in Fig. 5 below. The line segment O_1O_4 represents the position of the center line when the belt is empty, and the point is represented by $C_m(X_m, Y_m)$; At the maximum boundary of the belt deviation, the line segments O_2O_3 and $O_2'O_3'$ respectively indicate the right and left positions of the belt edge when the belt deviation is the maximum, AB and $A'B'$ are the right and left edge positions of the belt when the belt is empty, and the line segments MN and $M'N'$ They are the right and left edge positions of the belt in the current state detected by the Hough line detection method in the ROI area^[10]. Take the right side as an example. The coordinates at both ends of the line segment MN are represented by $N(X_0, Y_0)$ and $M(X_1, Y_1)$, the midpoint of the line segment AB is represented by $C_i(X_i, Y_i)$, and the midpoint of the line segment MN is represented by $C(\frac{X_0 + X_1}{2}, \frac{Y_0 + Y_1}{2})$. The midpoint O_2O_3 is represented by $C_{max}(X_{max}, Y_{max})$. The method of establishing the ROI area on the right side of the belt operation can be similar to the expression method of the ROI area on the left side of the belt operation.

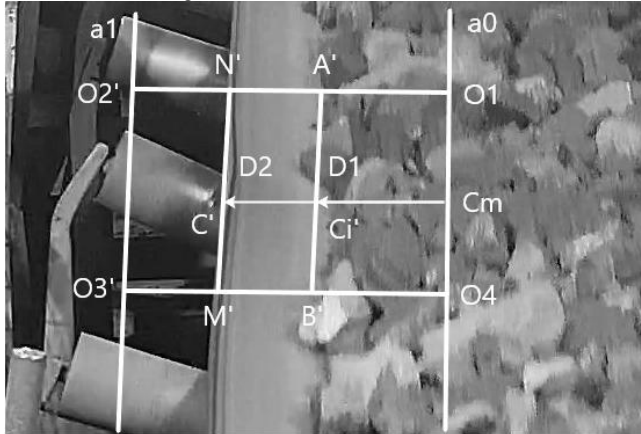
B. Mathematical model of belt deviation judgment

In the process of judging whether the belt is off-track, it is mainly to extract the effective features of the collected images, and compare the position of the belt when the belt is empty with the position when the belt is loaded, so as to achieve the purpose of judging whether the belt is off-track. This system adopts the method of analyzing the region of interest to reduce the detection range.

The distance from the edge position of the belt to the center line of the belt under no load is compared with the distance from the edge position of the belt to the center line of the belt



(a) ROI area of the right belt;



(b) ROI area of the left belt

Fig. 5. Belt edge detection image

under no load in the current state to determine whether the belt is off-track and the specific direction of deviation. That is to say, it can be simplified to compare the distances D_1 , D_2 between points C and C_i to C_m . Still take the selected right ROI area as an example: take the belt transportation direction as the positive direction. When $D_1 > D_2$, the belt is offset to the right, that is, select the right ROI area $O_1O_2O_3O_4$ to calculate the belt deviation percentage μ . Figure 5 (a) is the belt to the right-Side deviation, the percentage of belt deviation is expressed as

$$\mu = \frac{\sqrt{\left(\frac{X_0 + X_1}{2} - X_i\right)^2 + \left(\frac{Y_0 + Y_1}{2} - Y_i\right)^2}}{\sqrt{(X_{\max} - X_i)^2 + (Y_{\max} - Y_i)^2}} \times 100\% \quad (2)$$

When $D_1 < D_2$, the belt was shifted to the left, that is, the left ROI area $O_1'O_2'O_3'O_4'$ was selected to calculate the belt deviation percentage μ' . Figure 5(b) is the belt deviation to the left, the percentage of belt deviation is expressed as

$$\mu' = \frac{\sqrt{\left(\frac{X'_0 + X'_1}{2} - X'_i\right)^2 + \left(\frac{Y'_0 + Y'_1}{2} - Y'_i\right)^2}}{\sqrt{(X'_{\max} - X'_i)^2 + (Y'_{\max} - Y'_i)^2}} \times 100\% \quad (3)$$

The calculated belt deviation percentage is used to judge whether the belt is deviation, and the belt deviation degree is judged by observing the belt deviation percentage: normal state, slight deviation, severe deviation, and the judgment result is displayed on the monitoring interface.

V SPRINKLING JUDGMENT BASED ON SVM

In the process of judging whether the belt is sprinkled, the width of each area can be expressed by calculating the number of pixel coordinates of each area. When the belt is in a normal state, the width difference between the left and right sides without mineral material is relatively small; when the belt is misaligned, the difference in the width of the mineral-free area on the left and right sides of the belt is relatively large. Therefore, the width of the non-mineralized area at both ends of the belt can be used to judge whether the belt is sprinkled. Although the traditional judgment method can also achieve the purpose of detecting whether the belt is sprinkled, the process is too complicated and the anti-interference ability is not strong. Therefore, this paper uses support vector machines in machine learning to classify samples to improve the accuracy and efficiency of the system [11].

Support vector machine is a supervised learning model in machine learning, which can be used for data analysis, pattern recognition, and applied to classification and regression analysis. It is a typical two-class classification model [12]. Especially in the case of small samples, the support vector machine is constructed using the principle of structural risk minimization. The main idea of support vector machine is to find a hyperplane to distinguish two different types of samples [13]. Namely: construct input variables $x \in R^n$, output variables $y \in R$ and n-dimensional training sample sets $D = \{(x_1, y_1), (x_2, y_2), \dots, (x_n, y_n)\}$. In the n-dimensional space, find the hyperplane equation that best fits the input vector and output vector of the training sample $f(x) = \omega x + b$ (ω is the weight, b is the threshold) The problem can be transformed into

$$\min_{\omega, b} \frac{1}{2} \|\omega\|^2 \quad (4)$$

$$s.t. y_i(\omega x_i - b) \geq 1, i = 1, 2, L, l$$

To optimize the objective function, the Lagrange function is defined as follows

$$L(\omega, b, \alpha) = \frac{1}{2} \|\omega\|^2 + \sum_{i=1}^l \alpha_i [1 - y_i(\omega^T x_i + b)] \quad (5)$$

Where α_i is the Lagrange coefficient, $\alpha_i > 0$. Separate partial differentiation of ω , b in equation (5), then the problem is transformed into a quadratic programming maximum problem of finding the following function for α_i :

$$W(\alpha) = \sum_{i=1}^l \alpha_i - \frac{1}{2} \sum_{i,j=1}^l \alpha_i \alpha_j y_i y_j (x_i \cdot x_j) \quad (6)$$

$$s.t. \sum_{i=1}^l y_i \alpha_i = 0 \quad \omega = \sum_{i=1}^l y_i \alpha_i x_i \quad \alpha_i \geq 0$$

When the optimal solution α_i^* ($\alpha_i^* \neq 0$) is obtained, the corresponding sample is the support vector, and the output of the corresponding classification function $f(x)$ is the classification result:

$$f(x) = \text{sign} \left| \sum_i y_i \alpha_i (x_i \cdot x) - b \right| \quad (7)$$

In this design, x_i represents the pixel value of each point on the section line, and y_i represents the output sprinkling

result (0, 1, 2), that is, the degree of sprinkling (normal state, slight deviation, severe deviation) [14].

Choosing a relatively appropriate threshold D , the input of the SVM prediction model for belt running status monitoring is the pixel value on each section line, which constitutes the training sample of the SVM recognition model [15]. The whole process of SVM classification is as follows:

- 1) Collect data, select features, and input sample data into SVM;
- 2) Normalized data. Convert the value range of the sample data into a uniform interval;
- 3) The data set is divided into training set and test set;
- 4) Choose the appropriate kernel function;
- 5) Use cross-validation to find the best parameters C and γ ;
- 6) Train the entire training set with the best parameters C and γ obtained, thereby deriving the model;
- 7) Test: Use the test set to test the model and get the accuracy. This accuracy can be regarded as the final accuracy of the model. The calculation formula for accuracy is:

$$acc = \frac{1}{m} \sum_{i=1}^m (f(x_i) = y_i) \quad (8)$$

Where m represents the number of samples, $f(x_i)$ represents the predicted sample, and y_i represents the actual value;

- 8) Recognition classification: the formation of two hyperplanes means the formation of the objective function, which is then substituted into the sample to be recognized, the corresponding parameter value is entered in the recognition time, and the result is obtained and its category is judged [16].

VI TEST RESULTS AND EFFECTIVENESS ANALYSIS

Verify the method proposed above. Choose an appropriate threshold as the classification threshold of SVM. In order to compare the classification of the SVM algorithm, the number of training samples and the number of test samples selected in this paper are 500 and 100 respectively, and experiments are carried out on linear kernel function SVM, Gauss kernel function SVM and polynomial kernel function SVM. The data set is used as the input of linear kernel function SVM, Gaussian kernel function SVM and polynomial kernel function SVM. Through the analysis of the recognition results, it can be seen that the Gaussian kernel function SVM has the best recognition effect [17]. The recognition results are shown in TABLE I.

TABLE I
RECOGNITION RESULTS OF DIFFERENT ALGORITHMS

algorithm	Number of test samples	Recognition accuracy
Linear kernel function SVM	100	79.56%
Gaussian kernel function SVM	100	95.67%
Polynomial kernel function SVM	100	85.56%

The learning process of SVM replaces nonlinear mapping to high-dimensional space with inner product kernel function, and selects Gaussian kernel function:

$$k(x, x_j) = \exp\left(-\frac{\|x_i - x_j\|^2}{2\sigma^2}\right) \quad (9)$$

Among them, $\sigma > 0$ is the bandwidth of the Gaussian kernel function.

In order to verify whether the belt edge detection and mineral distribution state detection methods proposed by this system are feasible in practical applications, the system is used to detect the belt state in real time to test the performance of the system.

When the set value is exceeded, the system will display an early warning to remind the operator [18]. This information is real-time, and all detected data can be uploaded to the database. In order to improve the fault tolerance rate of the system, we divide a belt into multiple areas and detect them separately, and then combine the multiple detected results to obtain the final detection result according to a certain weight, and display it on the monitoring interface [19].

When designing the system, it is stipulated that when the belt deviation ratio is less than 15%, the belt is in a normal state; at this time, the system does not take warning. The operator can set the maximum belt deviation ratio by himself through the monitoring interface μ_{max} . When the detected belt deviation ratio exceeds this specified value, it is judged that the belt at this time is seriously deviated. By comparing the blank widths c_l, c_r of the left and right areas on the belt with the maximum widths c_{lm}, c_{rm} on the left and right sides set by the operator, it is judged whether the belt has the risk of spilling materials. Refer to TABLE II for specific criteria for judging failures.

TABLE II
FAILURE JUDGMENT CRITERIA

Fault classification	Judgments based
normal status	$0 < \mu < 15\%$
Slight deviation	$15\% < \mu < \mu_{max}$
Severe deviation	$\mu > \mu_{max}$
Sprinkle	$c_l < c_{lm}$ or $c_r < c_{rm}$

In order to verify the efficiency and feasibility of the system in actual application, the system's belt deviation and sprinkling detection functions were tested in different time periods in the ore processing plant, and the work of this system in the actual application process was observed. effect [20]. In the end, 5000 collected images were randomly selected to summarize and summarize, including 2700 images of belt under normal condition, 1200 images of detected deviation, 800 images of detected spatter, deviation + spill There are 300 images of the material. Compare the real situation observed with the results detected by the application of this system, summarized in TABLE III.

From Table III, it can be calculated that the false detection rate of this system is roughly 0.0667%, and the missed detection rate is roughly 0.0074%. We found that there were still 20 samples in normal condition that were mistakenly detected as misaligned + sprinkled samples. Through

research, we found that the reasons for this result are roughly as follows:

- 1) When the belt is misaligned, the distribution of minerals happens to be uneven, or the minerals There is too much distribution in a certain section of the belt so that the mineral material is too close to the edge of the belt and will be spilled. At this time, it is easy to be misjudged by the system as deviation + sprinkling;
- 2) When the belt deviation, the mineral material transported on the belt will fall off due to inertia. If it falls closer to the edge of the belt, the system is prone to misjudgment at this time;
- 3) The maximum belt deviation ratio set by the operator and other parameters will also have a certain impact on the accuracy of the system's judgment. If the parameters are set too high, the actual situation may not match the result detected by the system. Of course, this is also to reduce the missed detection rate, and to avoid failure of the belt due to incorrect correction of deviation during the working process, thereby reducing work efficiency. Or the uneven distribution of the mineral material causes a large amount of mineral material to fall, which causes a waste of resources. In general, this approach is to avoid belt failures due to deviations, reduce the risk of sprinkling, in order to minimize losses as much as possible.

VII CONCLUSION

The belt deviation and sprinkling detection system studied in this paper comprehensively uses image processing, edge detection and support vector machine methods. The Hough transform is used to locate the edge position of the belt, and the mathematical relationship between the belt position when loaded and the position of the belt when unloaded is used to judge the running state of the belt, and then the corresponding prompt is given on the operation interface. And users can set parameter values by themselves according to actual needs, which means that the system has a wide range of applications. At the same time, by constructing the SVM sprinkling forecast model, corresponding warning prompts are made on whether the belt is sprinkled or not. Experiments show that the SVM sprinkling detection model has zero false judgment rate and missed detection rate, and the detection accuracy is high. Through actual tests, it can be concluded that the system is practical, efficient, accurate, and stable. To

a certain extent, the system can ensure that the conveyor belt works more efficiently, reduce the burden on the staff, and lay the foundation for the realization of unattended conveyor belts.

REFERENCES

- [1] Nguyen Vanliem, Feng Dapeng, and Hou Lang, "Study on running deviation mechanism and intelligent control of belt conveyor," *Vibroengineering PROCEDIA*, vol. 36, pp6, 2021.
- [2] Mengchao Zhang, Hao Shi, Yan Yu, and Manshan Zhou, "A Computer Vision Based Conveyor Deviation Detection System," *Applied Sciences*, vol.10, no.7, 2020.
- [3] Chan Zeng, Junfeng Zheng, and Jiangyun Li, "Real-Time Conveyor Belt Deviation Detection Algorithm Based on Multi-Scale Feature Fusion Network," *Algorithms*, vol. 12, no.10, 2019.
- [4] Yanli Yang, Changyun Miao, Xianguo Li, and Xiuzhuang Mei, "On-line conveyor belts inspection based on machine vision," *Optik - International Journal for Light and Electron Optics*, vol. 125, no.19, 2014.
- [5] Zhu Liang Li Dongbo Wu Chongyou Wu Shaofeng Yuan Yanqiang, "Detection of belt deviation of belt weigher using data mining," *Editorial Office of Transactions of the Chinese Society of Agricultural Engineering*, vol. 33, no.1, pp8, 2017.
- [6] Qiu Yi Chu, Guo Ying Meng, and Xun Fan, "Analysis of Speed and Belt Deviation of the Conveyor Belt," *Advanced Materials Research*, vol.1453, 2011.
- [7] Lan Zhang, Lina Luo, Lei Hu, and Maohua Sun, "An SVM-Based Classification Model for Migration Prediction of Beijing," *Engineering Letters*, vol. 28, no.4, pp1023-1030, 2020.
- [8] Bardozzo Francesco, De La Osa Borja, Horanská Lubomíra, Fumanal-Idocin Javier, Priscoli Mattia delli, Troiano Luigi, Tagliaferri Roberto, Fernandez Javier, and Bustince Humberto, "Sugeno integral generalization applied to improve adaptive image binarization," *Information Fusion*, vol.68, pp9, 2021.
- [9] Chen Jiqing, Qiang Hu, Wu Jiahua, Xu Guanwen, and Wang Zhikui, "Navigation path extraction for greenhouse cucumber-picking robots using the prediction-point Hough transform," *Computers and Electronics in Agriculture*, vol.180, 2021.
- [10] Lin Chen, Dong Wei, and Jie-Sheng Wang, "Research on Magnetic Resonance Imaging Segmentation Algorithm," *Engineering Letters*, vol. 27, no.3, pp559-567, 2019.
- [11] Ma Liang, Jiang Hailin, Yang Wanli, and Zhu Quanjie, "A Novel Method to Identify Golgi Protein Types Based on Hybrid Feature and SVM Algorithm," *International Journal of Computational Intelligence and Applications*, vol.19, no.4, pp13, 2020.
- [12] Zhang Xiaoyuan, Li Chaoshun, Wang Xianbo, and Wu Huanmei, "A novel fault diagnosis procedure based on improved symplectic geometry mode decomposition and optimized SVM," *Measurement*, vol.173, 2021.
- [13] Shijin Kumar P.S., Udaya Kumar Naluguru, Ushasree A., and Sumalata G.L., "Key point oriented shape features and SVM classifier for content based image retrieval," *Materials Today: Proceedings*, 2020.
- [14] Qian Zhu, Yulin Luo, Dongyang Zhou, Yue-Ping Xu, Guoqing Wang, and Ye Tian, "Drought prediction using in situ and remote sensing products with SVM over the Xiang River Basin, China," *Natural Hazards*, pp25,2020.

TABLE III
TEST RESULTS OF BELT DEVIATION AND SPRINKLING DETECTION SYSTEM

Belt status	Number of pictures / pages				False detection rate/%	Missed detection rate/%
	Number of samples	Identified sample	Samples of false detection	Undetected sample		
normal	2700	2680	0	20	0.0000	0.0074
Run off	1200	1200	0	0	0.0000	0.0000
Sprinkle	800	800	0	0	0.0000	0.0000
Deviation + sprinkling	300	320	20	0	0.0667	0.0000
total	5000	5000	20	20	0.0667	0.0074

- [15] Ibai Roman, Roberto Santana, Alexander Mendiburu, and Jose A. Lozano, "In-depth analysis of SVM kernel learning and its components," *Neural Computing and Applications*, 2020.
- [16] Meng Meng Niu, Hao Yang, and Jing Xi Li, "Three-Dimensional Design and Finite Element Analysis of Belt Feeder," *Advanced Materials Research*, vol.2649, 2013.
- [17] Wu Zhao, "Study on the Steel Cord Belt Joint Monitoring Based on Force Displacement Curve," *Applied Mechanics and Materials*, vol.2802, 2014.
- [18] Jia Dong Dong, and Li Chen Gu, "Simulation of Hydraulic Servo System Based on Dynamic Monitoring in Mechanical Engineering," *Advanced Materials Research*, vol.2225, 2013.
- [19] Shuo Wen, Jie-Sheng Wang, and Jie Gao, "Fault Diagnosis Strategy of Polymerization Kettle Equipment Based on Support Vector Machine and Cuckoo Search Algorithm," *Engineering Letters*, vol. 25, no.4, pp474-482, 2017.
- [20] Cristian Duran-Faundez, Daniel G. Costa, and Vincent Lecuire, "Perimeter-based Calculation of Object Coverage in Multi-Camera Systems," *Engineering Letters*, vol. 24, no.4, pp384-391, 2016.



WENZHU WANG was born in Jilin Province, P. R. China, received the B.S. degree in Measurement and Control Technology and Instruments from University of Science and Technology Liaoning, Anshan, P. R. China, in 2018.

She is currently pursuing the M.S. degree in Control Science and Engineering with University of Science and Technology Liaoning, Anshan, P. R. China. Her research interest is image processing research.



SHAOCHUAN XU was born in Liaoning Province, P. R. China, received the B.S. degree in automation from University of Science and Technology Liaoning, Anshan, P. R. China, received the M.S. degree in control science and engineering from University of Science and Technology Liaoning, Anshan, P. R. China, in 1995, and 2004.

He is currently an associate professor in the School of Control Science and Engineering, University of Science and Technology Liaoning, Anshan, P. R. China. He published more than 20 academic papers, more than 20 patents and software copyrights. His research interests include research on industrial intelligent control and machine vision.



YUE TENG was born in Liaoning Province, P. R. China, received the B.S. degree in Measurement and Control Technology and Instruments from University of Science and Technology Liaoning, Anshan, P. R. China, in 2018, received the M.S degree in Control Science and Engineering from University of Science and Technology Liaoning, Anshan, P. R. China, in 2021.

Her research interests include image processing.